China Ocean Engineering, Vol.16, No.1, pp.89 – 105
 ISSN 0890-5487

Analysis of Wave Directional Spreading by Bayesian Parameter Estimation

Hwa CHIEN(钱桦)[a*], Laurence Z.H. CHUANG(莊士贤)[b] and Chia Chuen KAO(高家俊)[a]

[a]*Institute of Hydraulic and Ocean Engineering, Cheng Kung University, Tainan 80101, China*

[b]*Coastal Ocean Montioring Center, Cheng Kung University, Tainan 70101, China*

(Received 29 November 2001; accepted 28 December 2001)

ABSTRACT

A spatial array of wave gauges installed on an observatoion platform has been designed and arranged to measure the local features of winter monsoon directional waves off Taishi coast of Taiwan. A new method, named the Bayesian Parameter Estimation Method(BPEM), is developed and adopted to determine the main direction and the directional spreading parameter of directional spectra. The BPEM could be considered as a regression analysis to find the maximum joint probability of parameters, which best approximates the observed data from the Bayesian viewpoint. The result of the analysis of field wave data demonstrates the highly dependency of the characteristics of normalized directional spreading on the wave age. The Mitsuyasu type empirical formula of directional spectrum is therefore modified to be representative of monsoon wave field. Moreover, it is suggested that S_{max} could be expressed as a function of wave steepness. The values of S_{max} decrease with increasing steepness. Finally, a local directional spreading model, which is simple to be utilized in engineering practice, is proposed.

Key words: *directional wave spectrum*; *Bayesian theorem*; *wave age*

1. Introduction

The dramatic growth of land demands for industry has occurred over the past decade in Taiwan. Therefore, the Industry Bureau made great efforts to reclaim land from the sea. The Yuenlin reclamation industrial area, which is located on the western coast of Taiwan, is the largest piece. The total area of Yuenlin reclamation industrial area in the design is 10580 hectares. It is obvious that the construction of the reclamation project will affect the sea states and cause topographical changes nearby, or even may result in disasters. Among all the oceanographic factors, ocean wave is the most dominant and complicated one. Ocean waves, which make a feature of extremal randomness, are directly and indirectly dependent on mateorological, hydrological, oceanographic, and topological factors. They cannot be fully understood only by theoretical approaches. In order to strengthen the sustainable development in the coastal zones, field measurement must be performed to increase the knowledge of the characteristics of local waves. The Coastal Ocean Monitoring Center at Cheng Kung University is entrusted with the duty of collecting oceanographic information in this area. In consideration of severe weather and sea conditions, a spatial array of wave gauges installed on an observation platform is designed and arranged to measure the local features of directional wave off Taishi coast of Yuenlin county.

* Corespending author; e-mail: n8885105@ccmail.ncku.edu.tw

The directional spectrum can be expressed as the product of the directional spreading function and the frequency spectrum. The directional spreading can be separately computed for each frequency. In the estimation of wave directionality, several methods have been developed, such as Fourier Series Method (FSM), Maximum Likelihood Method(MLM), Maximum Entropy Method(MEM), Bayesian Directional Method(BDM), and their modifications. The directional spreading functions of the above-mentioned methods are derived based on various theories and have diverse characteristics. Comparisons (Kim *et al*., 1994) through numerical simulations demonstrate that different methods give different directional spreading even when they are applied to the same data set. On the other hand, long-term measurements need to be analyzed and represented by directional spectral models instead of individual estimated spectrum before they are offered as reference for engineering design. This process of data fitting may bring the errors. In order to obtain the overall characteristics of the directional spectra of winter monsoon waves and to improve the resolution of directional spreading and the stability of operational computation, the present study aims to firstly develop the estimator of the parameters in the directional spectral model and secondly to discuss and modify the model. A new method, named the Bayesian Parameters Estimation Method (BPEM), is proposed for estimating parameters of the directional spreading function of random waves from an array of wave probes. The BPEM is then applied to field data obserbed at Taishi. The results of analysis are compared with Mitsuyasu's empirical formula for investigation of the characteristics of directional spreading.

2. Fundamental Equations of Directional Spectrum Analysis

The directional spectrum can be derived by cross-power spectrum, which is the Fourier transformation of covariance function of any two measured wave properties. The general relationship between the cross-power spectrum, $\Phi_{mn}(f)$, for a pair of arbitrary wave properties, and the directional spectrum, $G(f,\theta)$, derived by Isobe and Horikawa (1984), is:

$$\Phi_{mn}(f) = \int_0^{2\pi} H_m(f,\theta)\overline{H}_n(f,\theta)\cdot[\cos\{k(X_{mn}\cos\theta + Y_{mn}\sin\theta)\} - i\sin\{k(X_{mn}\cos\theta + Y_{mn}\sin\theta)\}]G(f,\theta)\mathrm{d}\theta \quad (1)$$

where f is frequency; k is wave number; i is imaginary unit; X_{mn} and Y_{mn} are the distance between the m-th and the n-th wave properties in the coordinates(X, Y). $\overline{H}(f,\theta)$ denotes the complex conjugate of $H_n(f,\theta)$, and $H_m(f,\theta)$ is the transfer function.

The directional spectrum is often expressed as a product of the frequency spectrum $S(f)$ and the directional spreading function $D(\theta|f)$.

$$G(f,\theta) = S(f)\cdot D(\theta\mid f). \quad (2)$$

The directional spectrum takes non-negative values and satisfies the following relationship:

$$\int_0^{2\pi} G(f,\theta)\mathrm{d}\theta = S(f). \quad (3)$$

Substitution of the above equation into Eq.(3) yields

$$\int_0^{2\pi} D(\theta \mid f) = 1. \tag{4}$$

For simplification of the nomenclature in the equations, Eq. (1) is rewritten by Hashimoto in the following form:

$$\psi_i(f) = \int_0^{2\pi} h_i(f,\theta) D(\theta \mid f) \mathrm{d}\theta, \quad (i = 1, \cdots, N), \tag{5}$$

where N is the number of equations, and

$$h_i(f,\theta) = H_m(f,\theta)\overline{H}_n(f,\theta) \cdot [\cos\{k(X_{mn}\cos\theta + Y_{mn}\sin\theta)\} - i\sin\{k(X_{mn}\cos\theta + Y_{mn}\sin\theta)\}]/W_{mn}(f). \tag{6}$$

$$\psi_i(f) = \frac{\Phi_{mn}(f)}{\overline{S}(f) \cdot \overline{W}_{mn}(f)}, \quad D(\theta \mid f) = G(f,\theta)/S(f), \tag{7}$$

in which $W_{mn}(f)$ is a weighting function introduced for normalizing and non-dimensionalizing the errors of the cross-power spectra.

3. Proposed BPEM for Estimating Directional Distribution

3.1 Bayes' Theorem

The basic reasoning used in the present study is a straightforward application of Bayes' theorem denoted by the following equation:

$$P(H \mid DI) = P(H \mid I)\frac{P(D \mid HI)}{P(D \mid I)}. \tag{8}$$

In our problems, H is any hypothesis to be tested; D is the data; and I is the prior information. For construction of the likelihood the difference is taken between the model H function and the data D.

$$D_i = y(t_i) = H_i + e_i, \quad i = 1,2,\cdots,N. \tag{9}$$

If the true signal is known, then this difference would be just the noise. The least informative prior probability of the noise has a Gaussian form as follows:

$$P(e_i \mid I) = \frac{1}{\sqrt{2\pi\sigma^2}}\exp\left[\frac{-e_i^2}{2\sigma^2}\right] \tag{10}$$

where a new parameter σ^2 (the variance of the noise) is introduced. In the next step, the product rule from probability theory is applied to obtain the probability of a set of noise values $\{e_1, e_2, \cdots, e_N\}$:

$$P(e_1, e_2, \cdots, e_N) = \prod_{i=1}^{N}[P(e_i \mid I)] = (2\pi\sigma^2)^{\frac{-N}{2}}\exp\left\{\frac{-1}{2\sigma^2}\sum_{i=1}^{N} e_i^2\right\}. \tag{11}$$

And the probability is proportional to the likelihood function:

$$P(D \mid HI) = L(H) \propto (2\pi\sigma^2)^{\frac{-N}{2}}\exp\left[\frac{-1}{2\sigma^2}\sum_{i=1}^{N}(D_i - H_i)^2\right]. \tag{12}$$

One of the approaches to further processes is to minimize the sum in the exponent, so as to obtain the corresponding parameters. The previous problem can be simplified by substituting Eq. (12) into Eq. (8) to absorb the influence of the term $P(D|I)$ into the normalization constant. The simplified relationship with respect to H for given realized sample data D is:

$$P(H \mid DI) \propto P(D \mid HI)P(H \mid I) = L(H)P(H \mid I) \tag{13}$$

3.2 Formulation of Directional Spectral Estimation

For estimation of the directional spreading, it is firstly assumed that the directional spreading function can be expressed as a piecewise-constant function over the directional range from 0 to 2π ($k\Delta\theta = 2\pi$). Eq.(5) could then be approximated by the following equation.

$$\psi_i(f) = \sum_{k=1}^{K} G_k(f) \int_0^{2\pi} h_i(f,\theta) \cdot I_k(\theta) \mathrm{d}\theta \tag{14}$$

in which

$$I_k(\theta) = \begin{cases} 1 & (k-1)\Delta\theta \leqslant \theta \leqslant k\Delta\theta \\ 0 & \text{otherwise} \end{cases} \qquad k = 1,2,\cdots,K \tag{15}$$

and

$$G_k(f) = D(\theta_k \mid f). \tag{16}$$

If the value K is large enough, the integral of the right hand side of Eq.(14) can be further approximated by the following equation.

$$\int_0^{2\pi} h_i(f,\theta) \cdot I_k(\theta) \mathrm{d}\theta = \int_{(k-1)\Delta\theta}^{k\Delta\theta} h_i(f,\theta) \cdot I_k(\theta) \mathrm{d}\theta \approx h_i(f,\theta_k)\Delta\theta \equiv \alpha_{i,k}(f). \tag{17}$$

Eq.(14) can be then expressed as,

$$\psi_i(f) = \sum_{k=1}^{K} \alpha_{i,k}(f) \cdot G_k(f), \quad i = 1,2,\cdots,N. \tag{18}$$

Herein, the complex numbers are written in the following forms,

$$\left.\begin{aligned} \varphi_i(f) &= \mathrm{Re}[\psi_i(f)] & \varphi_{N+i}(f) &= \mathrm{Im}[\psi_i(f)] \\ \alpha_{i,k}(f) &= \mathrm{Re}[\alpha_{i,k}(f)] & \alpha_{N+i,k}(f) &= \mathrm{Im}[\alpha_{i,k}(f)] \end{aligned}\right\}. \tag{19}$$

When Eq.(18) is applied to the observed data, the error contained in the data must be taken into account. Eq.(20) is the modification of Eq.(18) considering the existence of errors.

$$\varphi_i = \sum_{k=1}^{K} \alpha_{i,k} G_k + e_i, \quad i = 1,2,\cdots,2N. \tag{20}$$

3.3 Estimation of Unimodal Directional Spreading

The unimodal directional spreading function adopted in the present study is proposed by Longuet-Higgins *et al*. (1963). S is the well-known spreading parameter demonstrating the width of the directional spreading and θ is the dominant wave direction:

$$G_k = A\cos^{2S}\left[\frac{\theta_k - \theta}{2}\right], \quad k = 1,2,\cdots,K. \tag{21}$$

For the given $\varphi_i (i = 1,2,\cdots,2N)$, the likelihood function of $G_k (k = 1,2,\cdots,K)$ and σ^2 could be derived from Eq.(13) and can be expressed as

$$L(S,\theta,A,\sigma) = (2\pi\sigma^2)^{-N} \exp\left[\frac{-1}{2\sigma^2} \sum_{i=1}^{2N} \left(\varphi_i - \sum_{k=1}^{K} \alpha_{i,k} G_k\right)^2\right]$$

$$= (2\pi\sigma^2)^{-N}\exp[\frac{-Q}{2\sigma^2}] \tag{22}$$

in which

$$Q = \sum_{i=1}^{2N}\Big\{\varphi_i^2 - 2A\varphi_i\sum_{k=1}^{K}\alpha_{i,k}\cos^{2S}(\frac{\theta_k-\theta}{2}) + A^2\sum_{k=1}^{K}\sum_{l=1}^{K}\alpha_{i,k}\alpha_{i,l}\cdot\Big[\cos(\frac{\theta_k-\theta}{2})\cos(\frac{\theta_l-\theta}{2})\Big]^{2S}\Big\}$$
$$= 2N\bar{\varphi}^2 - 2A\cdot R(S,\theta) + A^2\cdot C(S,\theta)$$
$$= 2N\bar{\varphi}^2 - \frac{R^2}{C} + C\cdot(A-\frac{R}{C})^2 \tag{23}$$

and

$$\bar{\varphi}^2 = \frac{1}{2N}\sum_{i=1}^{2N}\varphi_i^2; \tag{24}$$

$$R(S,\theta) = \sum_{i=1}^{2N}\varphi_i\Big[\sum_{k=1}^{K}\alpha_{ik}\cos^{2S}(\frac{\theta_k-\theta}{2})\Big]; \tag{25}$$

$$C(S,\theta) = \sum_{i=1}^{2N}\Big\{\sum_{k=1}^{K}\sum_{l=1}^{K}\alpha_{ik}\alpha_{il}\Big[\cos(\frac{\theta_k-\theta_m}{2})\cos(\frac{\theta_l-\theta}{2})\Big]^{2S}\Big\}. \tag{26}$$

Substitution of the above into Eq. (22) gives

$$L(S,\theta,A,\sigma) = (2\pi\sigma^2)^{-N}\exp\Big\{\frac{-1}{2\sigma^2}\Big[2N\bar{\varphi}^2 - \frac{R^2}{C}\Big]\Big\}\cdot\exp\Big\{\frac{-C}{2\sigma^2}\Big[A-\frac{R}{C}\Big]^2\Big\}. \tag{27}$$

The problem to be solved is to compute the probability of the parameters S and θ conditional on the data and the prior information; this is abbreviated as $P(S,\theta\mid DI)$. However, difficulty arises due to the existence of two other parameters, A and σ in Eq. (27). These two parameters are referred to as nuisance parameters, because the probability distribution to be calculated does not depend on them. To eliminate the nuisance parameters, Bayes' theorem is applied and then integrating over A gives

$$P(S,\theta,\sigma\mid D,I) = \int P(S,\theta,A,\sigma\mid D,I)\mathrm{d}A \propto \int P(S,\theta,A,\sigma\mid I)\cdot P(D\mid S,\theta,A,\sigma,I)\mathrm{d}A. \tag{28}$$

In Eq. (28), no prior information about the parameter A is assumed. This indicates that the location parameter is completely ignorant, which contributes to a uniform, flat prior density. The posterior probability density for parameters S,θ, and σ is proportional to

$$P(S,\theta,\sigma\mid D,I) \propto \frac{\sigma^{-2N+1}}{\sqrt{C}}P(S,\theta,\sigma\mid I)\cdot\exp\Big\{\frac{-1}{2\sigma^2}\Big[2N\bar{\varphi}^2 - \frac{R^2}{C}\Big]\Big\}. \tag{29}$$

The above equation is depend on the variance of the noise, however, frequently one has no independent knowledge of the noise. The noise variance σ^2 then becomes a nuisance parameter. A Jeffreys prior, $1/\sigma$, is adopted to eliminate the nuisance paranmeter. Multiplying Eq. (29) by the Jeffreys prior and integrating over all positive values σ gives

$$P(S,\theta\mid D,I) \propto \frac{P(S,\theta\mid I)}{\sqrt{C}}\Big[2N\bar{\varphi}^2 - \frac{R^2}{C}\Big]^{-N+\frac{1}{2}}. \tag{30}$$

By taking logarithm we have

$$P(S,\theta \mid D,I) \propto \log[P(S,\theta \mid I)] + \frac{1}{2}\left[(1-2N)\log(2N\bar{\varphi}^2 - \frac{R^2}{C})^2 - \log C\right]. \quad (31)$$

If the prior probability $P(S,\theta \mid I)$ of the parameters S and θ is the same, a criterion named Log Posterior Probability of Parameters ($LPPP$) could be defined

$$LPPP = (2N-1)\log(2N\bar{\varphi}^2 - \frac{R^2}{C}) + \log C. \quad (32)$$

The most suitable values of the spreading parameter S and the mean direction θ are determined by minimization of the $LPPP$.

3.4 Validation by Numerical Simulation

To identify the validity of this method, numerical simulations have been performed. The procedures of the simulation are as follows: first, set a target directional spectrum; second, construct the cross spectra from the target spectra by use of Eq.(1); third, apply BPEM to the cross spectra and estimate the directional spectra. In the numerical simulations, 3 different arrangements of wave gauge arrays have been used, as shown in Fig. 1a to Fig. 1c. The JONSWAP spectrum and the Mitsuyasu type wave directional spreading are employed. i.e.

$$G(\theta \mid f) = G_0 \cos^{2s}\frac{\theta - \theta_0}{2}. \quad (33)$$

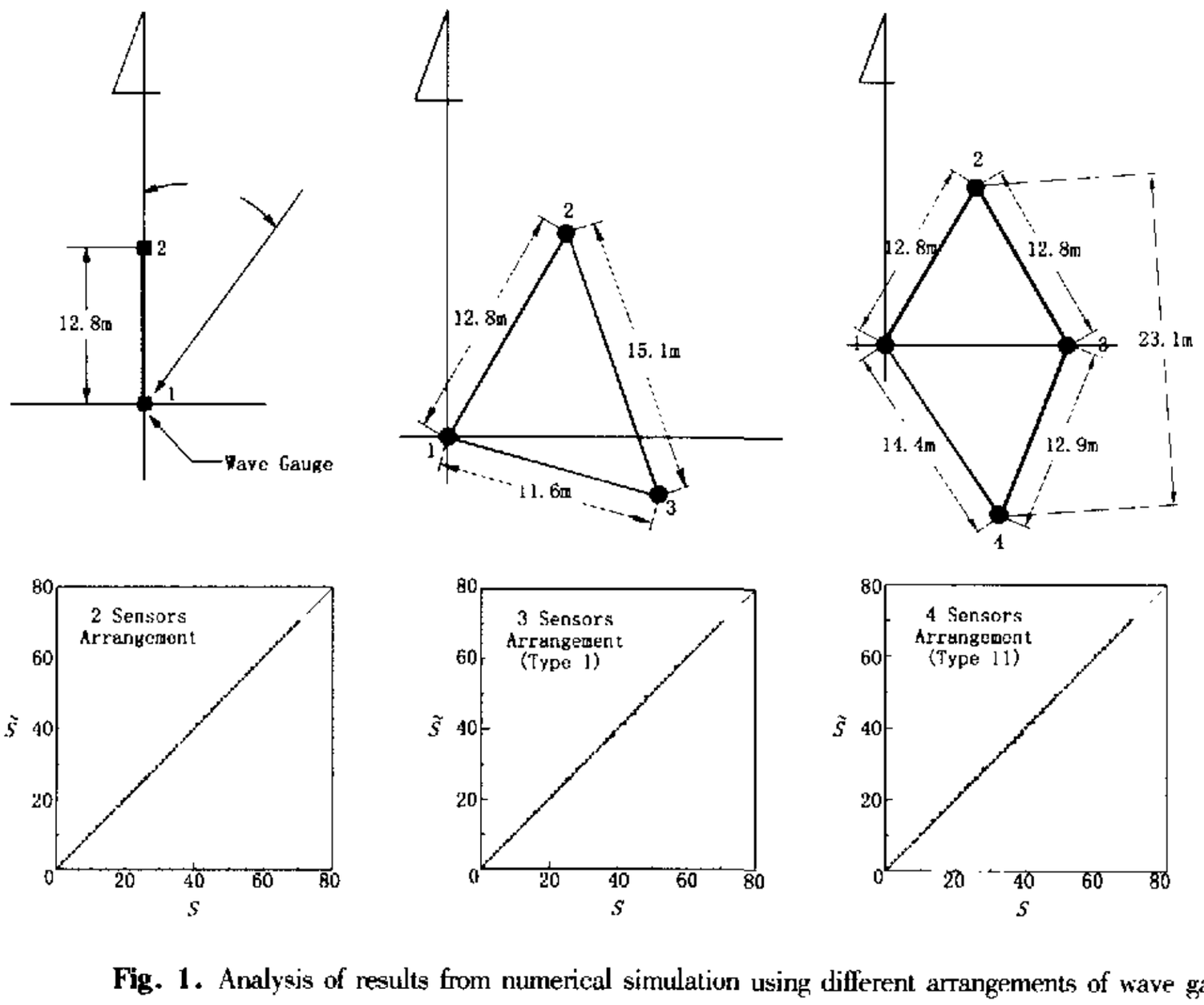

Fig. 1. Analysis of results from numerical simulation using different arrangements of wave gauges: (a)Two gauge array, (b)Triangular gauge array, (c)Quadrate gauge array.

The comparisons of results are illustrated in Fig. 1a to Fig. 1c. It is shown that the spreading parameter $\bar{S}$ can be accurately estimated with respect to a complete range of S in different arrangements of gauge arrays. As to the effect of the number of wave gauges in the array, it is found that the wave directionality can be retrieved even when only two wave gauges are applied. Owing to the limited wave information from the gauges of the sea surface, the wave directional spectrum could be only approximated. The more gauges provide more information and introduce less error. From the results, BPEM might be applied to few wave gauges and give similar results. Theoretically, that might be an advantage of reducing the cost of directional wave measurement. Considering the complexity of real field waves, however, the effect of the number of wave gauges in array in the field should be further investigated.

The Gaussian distribution and the Maximum Entropy Spreading, derived by Hashimoto *et al.*, are also utilized to simulate wide and narrow spreading respectively. The estimated results are compared with the target spreading in Fig. 2a and Fig. 2b. It is demonstrated that the BPEM is valid for analysis of simulated cross spectra in both wide and narrow directional energy distribution.

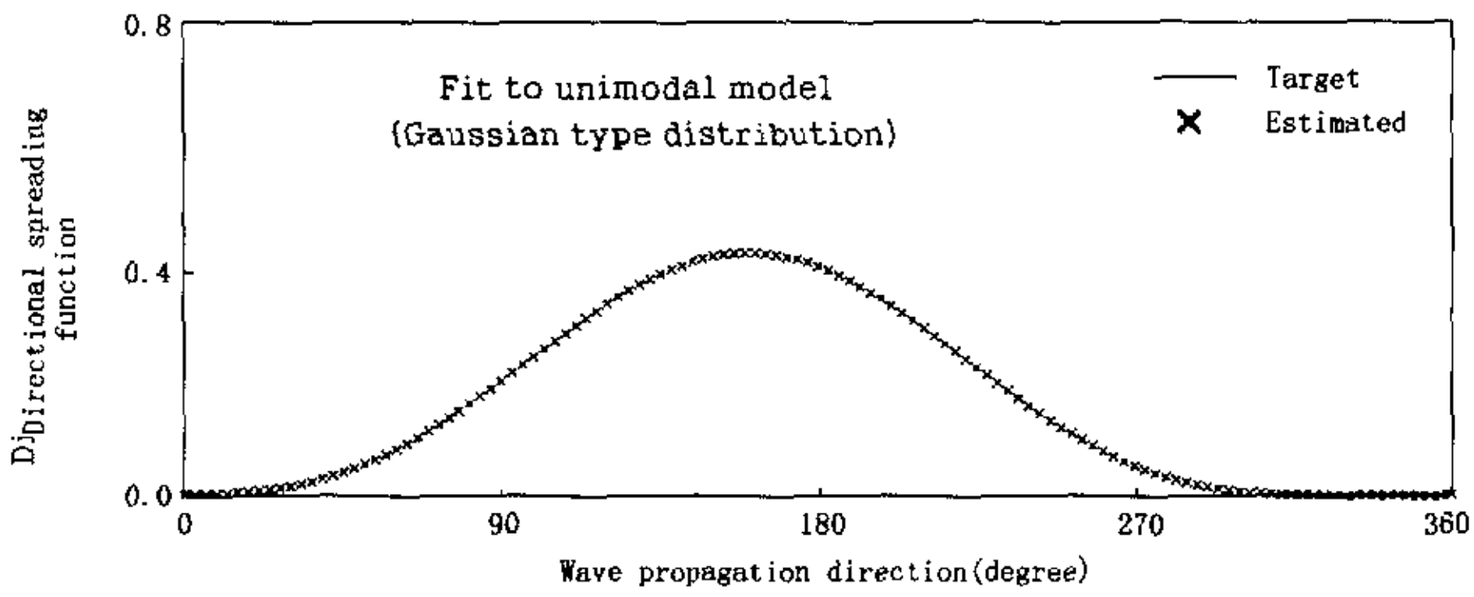

Fig. 2a. Comparison of target wide spreading and results estimated by BPEM.

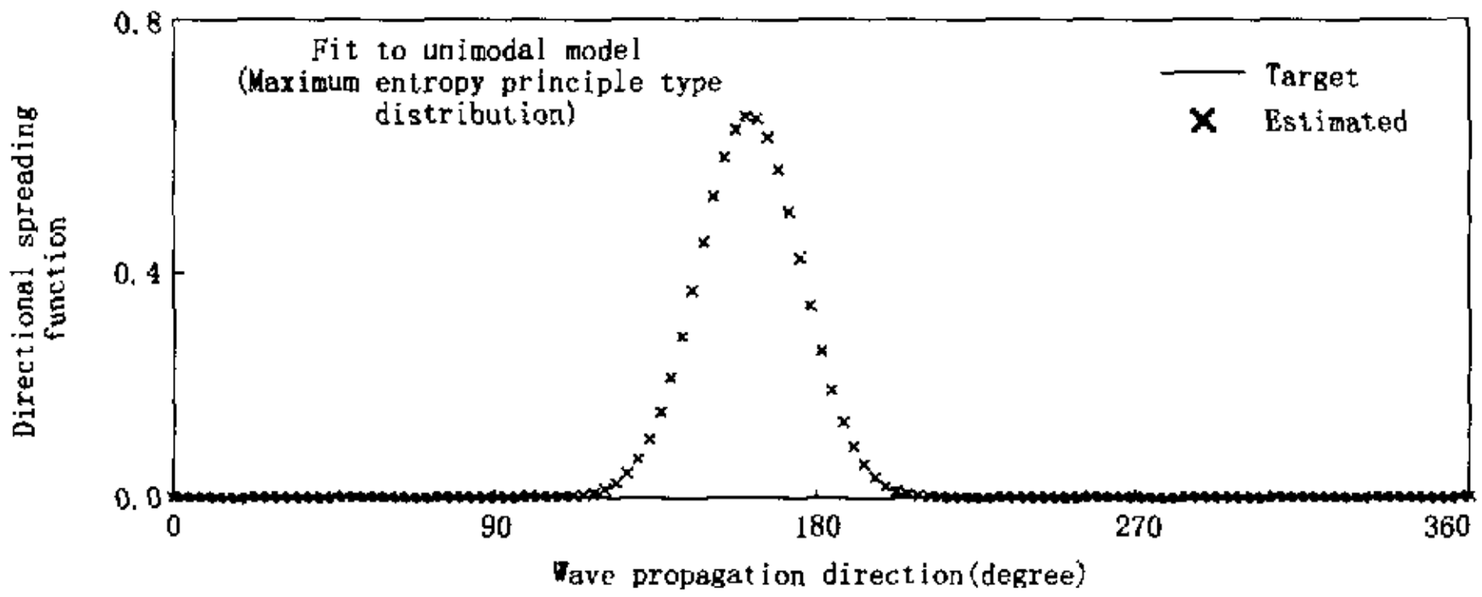

Fig. 2b. Comparison of target narrow spreading and results estimated by BPEM.

4. Analysis of Field Data

4.1 Data Acquisition

The Bayesian Parameter Estimation Method(BPEM) outlined in the previous section is then applied to the field data acquired at an observation platform, about 4 km off the Taishi coast, the middle-western coast of the Taiwan Island. The station is located at 23°45′39″N and 120°09′10″E, as shown in Fig.3. The average water depth is 15 meters, the local tidal range being about 2.5 meters. The bathymetric change in the neighborhood of the platform is rather flat. The average slope is 1/700. There is no topographic shelter in the north, which is the dominant wind direction for the winter monsoon season.

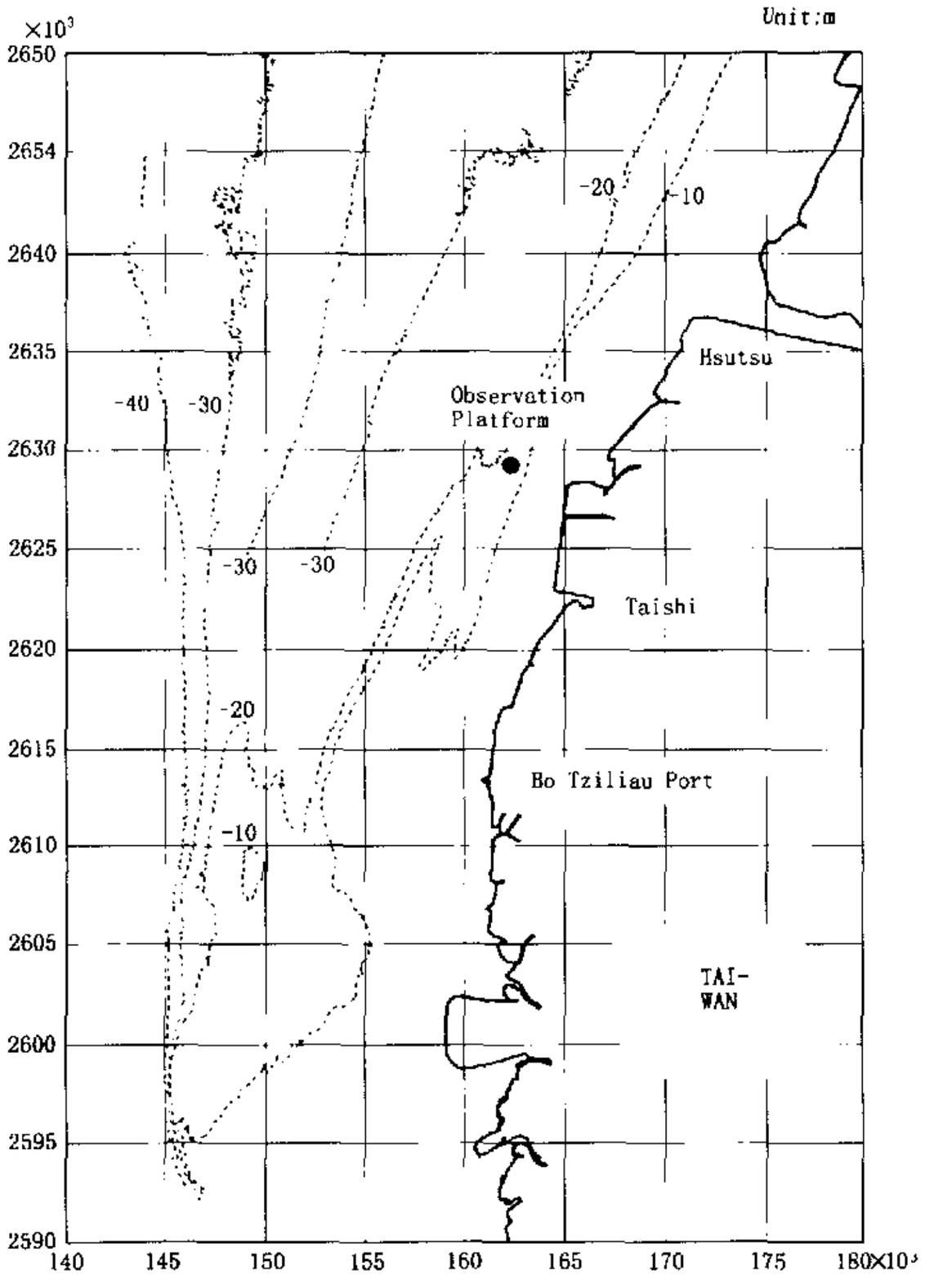

Fig. 3. Bathymetric map of the neighborhood area of Taishi platform station.

There are four ultrasonic wave gauges mounted at fixed positions extending from the four corners of the platform deck. The layout of the platform is illustrated in Fig.4. The ultrasonic wave gauges are arranged in an irregular quadrilateral, as shown in Fig.5. The shortest distance between every two gauges is

3.83 m, while the longest is 7.20 m. The simultaneous measurement of four wave elevations is performed over 20 minutes every 4 hours at a sample rate of 5 Hz.

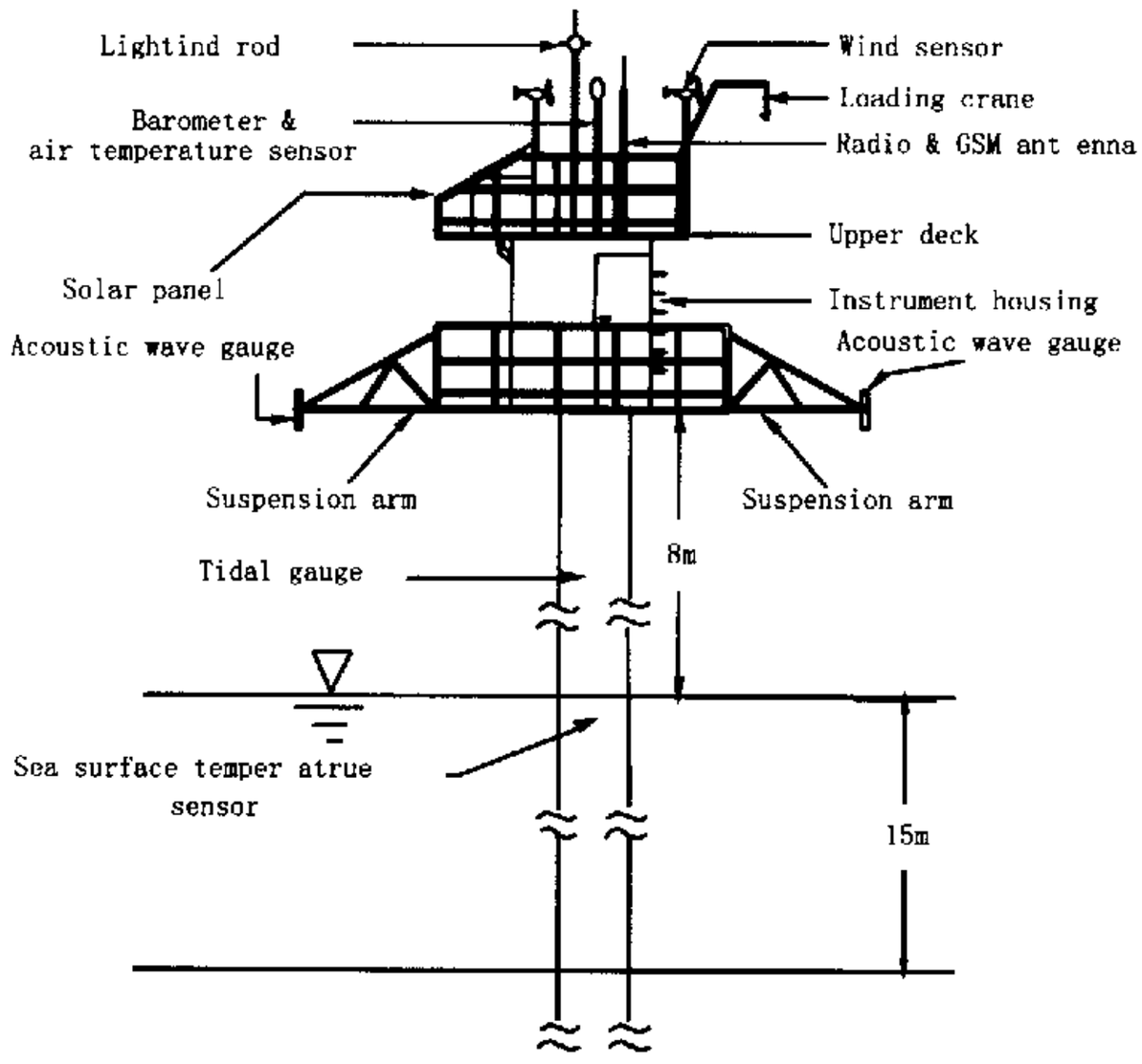

Fig. 4. Layout of Taishi platform station.

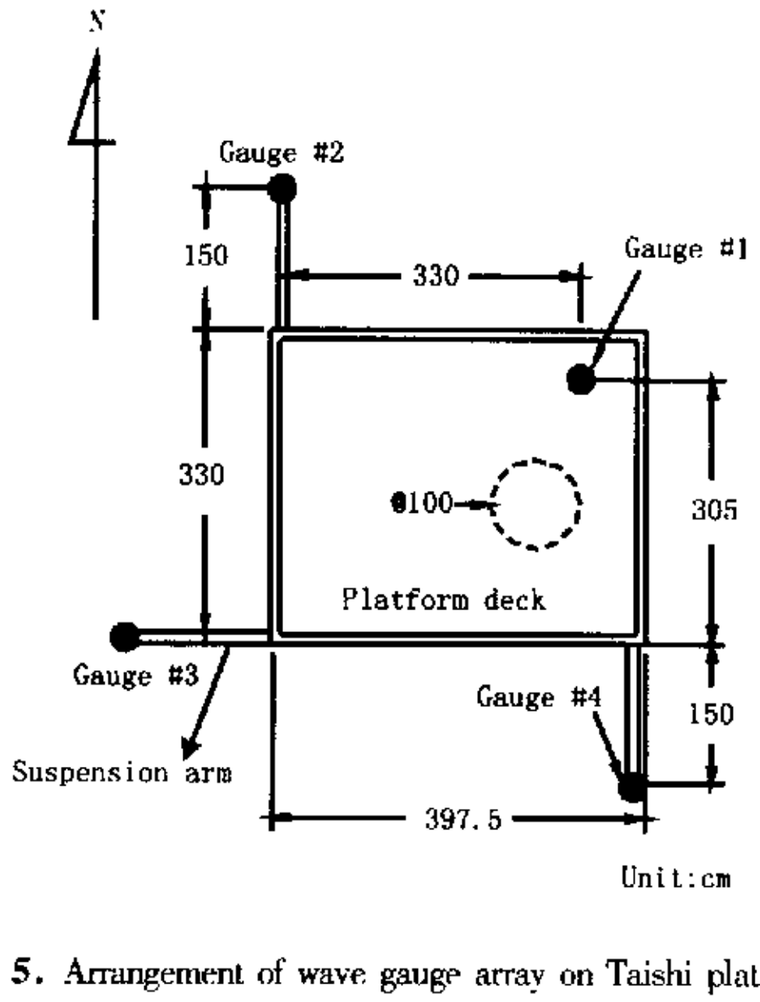

Fig. 5. Arrangement of wave gauge array on Taishi platform.

The sea states are dominated by the prevailingly north easterly monsoon in the Taiwan Strait during the winter season. A population of 413 records of northeasterly spectra is established by selecting all those spectra for which the wind and the mean wave direction are steady, and from the northeast during the period from December 1993 to February 1994. The area could be regarded as finite water depth since 80% of the wave frequencies range from 0.12 Hz to 0.2 Hz. To ensure the validity of the results from directional spectral analysis, data quality check is performed. Based on the ergodic process assumption, a subgroup is selected depending on the criterion that the coherence function of frequency spectra measured between gauges is higher than 0.8. The coherence function γ^2_{xy} is expressed as

$$\gamma^2_{xy}(f) = \frac{|\Phi_{xy}(f)|^2}{\Phi_{xx}(f) \cdot \Phi_{yy}(f)}. \tag{34}$$

Fig. 6a demonstrates one example of the frequency spectra and corresponding coherence functions that pass the data quality control, while Fig. 6b is an example of unqualified data set. This selection pro-

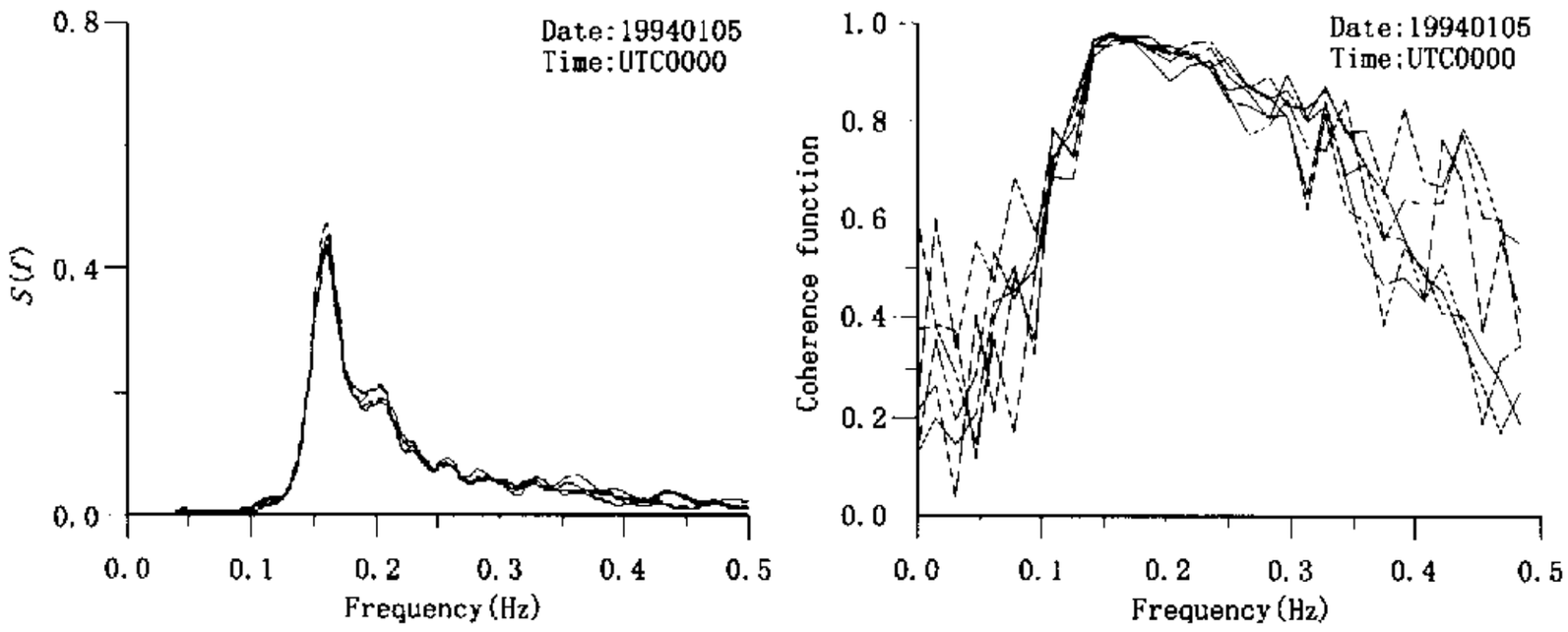

Fig. 6a. Example of frequency spectra and corresponding coherence functions of qualified data from the gauge array on Taishi platform.

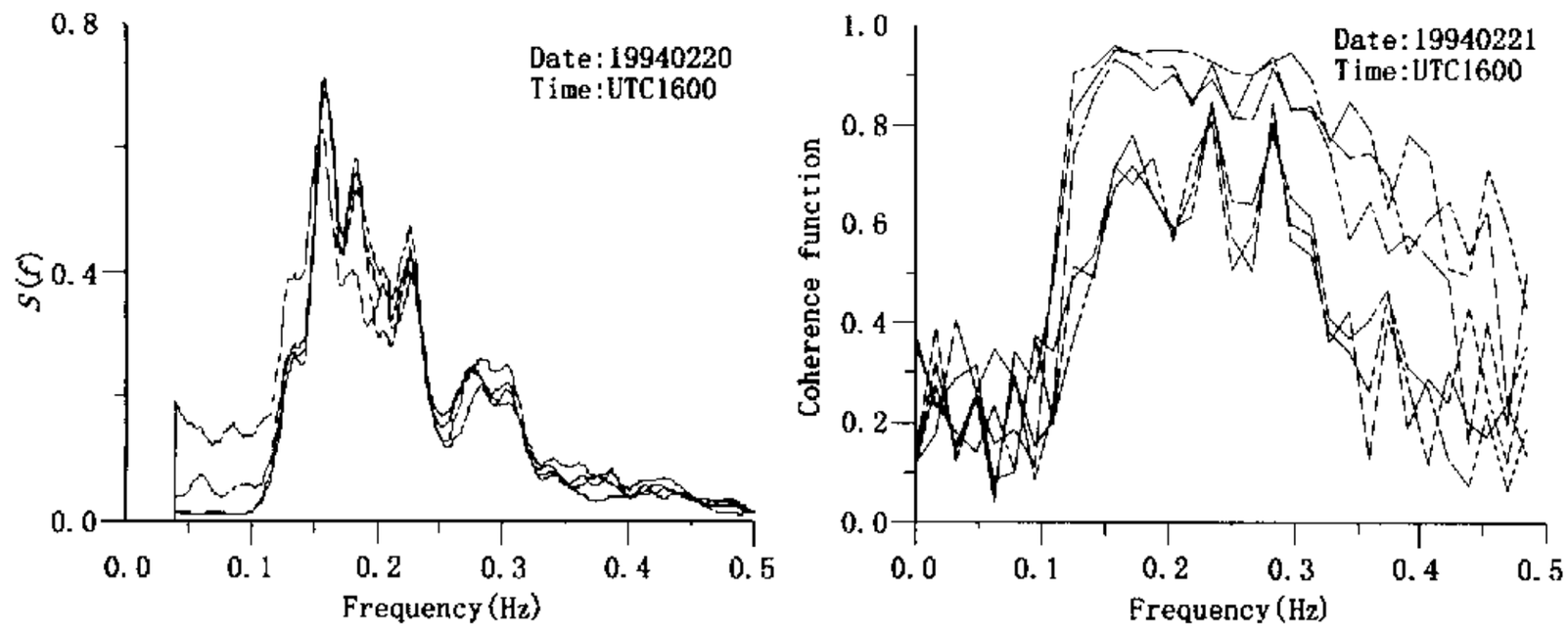

Fig. 6b. Example of frequency spectra and corresponding coherence functions of unqualified data from the gauge array on Taishi platform.

cess results in 183 sets of qualified field data. The results show that the waves propagate mainly from the northwest and northwest-by-north direction. In the discussion of the parameterization of S, data with higher wave height is focused; therefore waves with significant wave height larger than 1.5 m are selected. Finally, 64 sets of data are used.

4.2 Estimation of Directional Spreading Function

The directional spreading function to be estimated is assumed to be an unimodal form of Eq.(21). Then *LPPP*, which is defined as Eq.(32), could be applied to the determination of the main direction and the directional spreading parameter of directional spectra.

Fig. 7 gives the distribution of normalized spreading parameter, S/S_{max}, against the normalized frequency, f/f_P, for the selected wave records. According to the data measured by a cloverleaf buoy, Mitsuyasu *et al*.(1975) developed a relationship between S and the wave frequency, i.e.

$$S = \begin{cases} S_{max}(f/f_p)^5 & f \leqslant f_p \\ S_{max}(f/f_p)^{-2.5} & f > f_p \end{cases} \tag{35}$$

The lines with slopes of -2.5 and 5, representing Eq.(35), are also shown in Fig.7. The distribution of data points has the same tendency as previous observations that directional concentration has the maximum value at the spectral peak and decreases at both sides of the spectral peak. However, data scatter compared to Mitsuyasu's formula indicates the complexity of S.

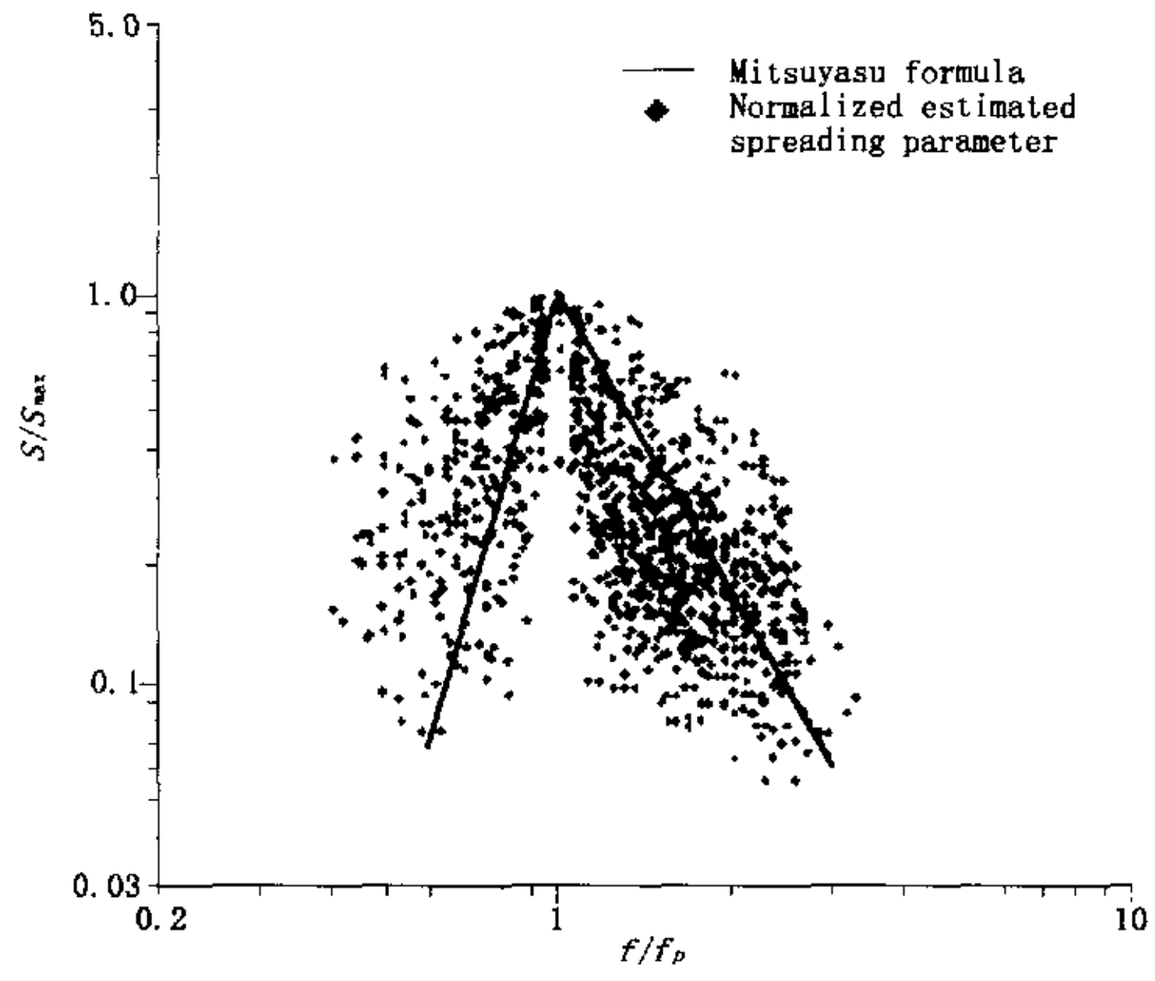

Fig. 7. Comparison of Mitsuyasu's model and estimated distribution of normalized S on non-dimensional frequency.

To investigate whether there are other factors influencing the characteristics of normalized spreading

parameter, it is assumed that S might be related to wave age or S_{max}. Therefore, data sets are categorized into 3 subgroups according to the values of respective S_{max}. It can be found in Fig.8 that scatter still exists. Since the measured wave data covers a wide range of wave age, the analyzed data are then categorized into 4 subgroups according to the values of corresponding wave age. Data sets with different ranges of wave age are shown in Fig.9a to Fig.9d, which demonstrate the relationship of normalized S and nondimensional frequency for each subgroup. It is found that the data scatter is significantly reduced of the relationship between normalized S and nondimensional frequency is classified into subgroups. Further

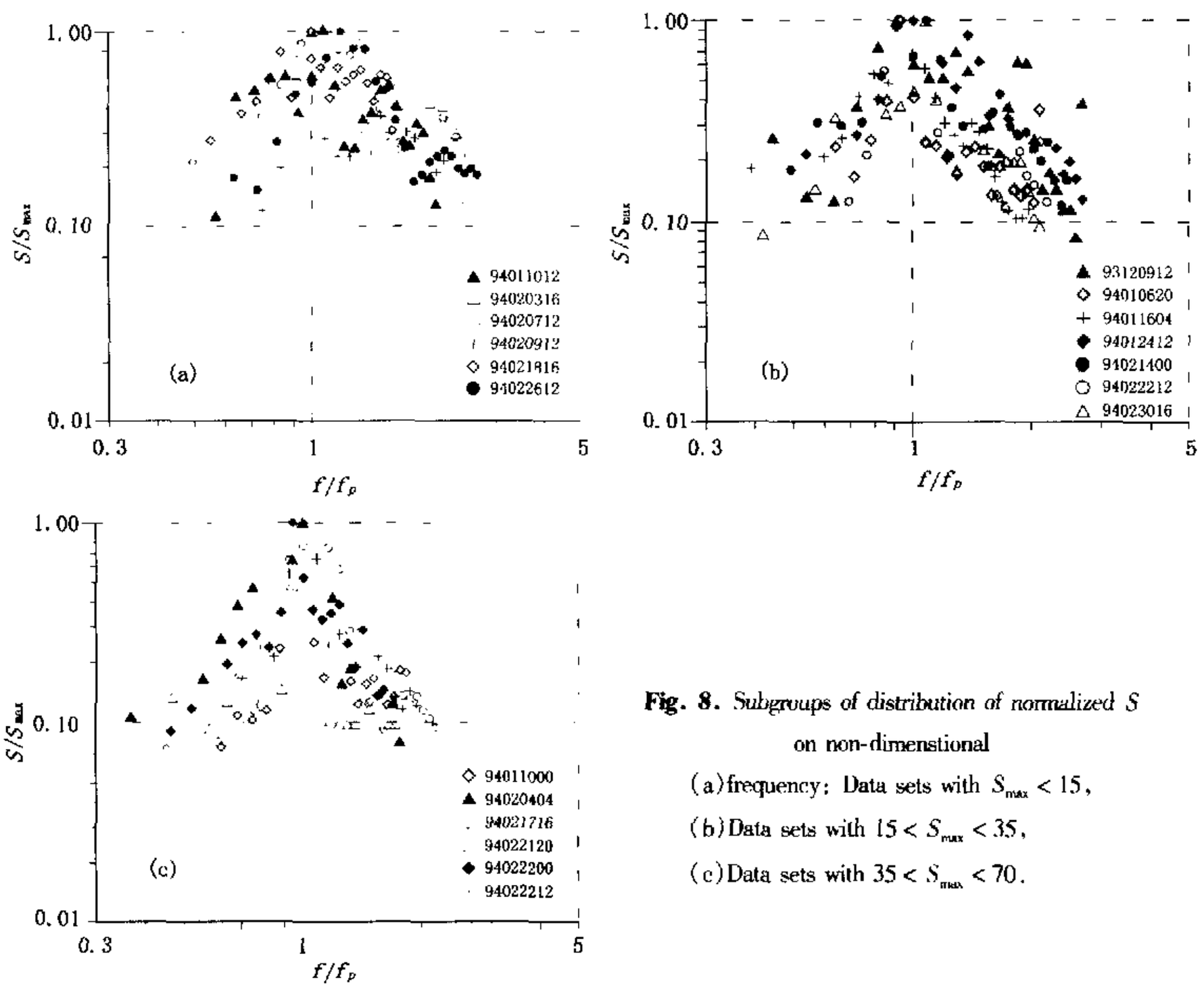

Fig. 8. *Subgroups of distribution of normalized S on non-dimenstional frequency: Data sets with $S_{max} < 15$, (b) Data sets with $15 < S_{max} < 35$, (c) Data sets with $35 < S_{max} < 70$.*

more, it is obvious that the slopes in subgroups (b), (c), and (d), in which the wave ages are larger then 1, vary depending on the wave age. The slopes become steeper in higher frequency, and milder in lower frequency with increasing wave age. Moreover, the dependency is stronger in the lower frequency than in the higher frequency. This finding would suggest that instead of constants of -2.5 and 5, the exponents in Mitsuyasy's formula might be the function of wave age. Fig. 10 shows the dependency of the parameters on the wave age. Linear regression is then performed to have a modified Mitsuyasu's formula, i.e.:

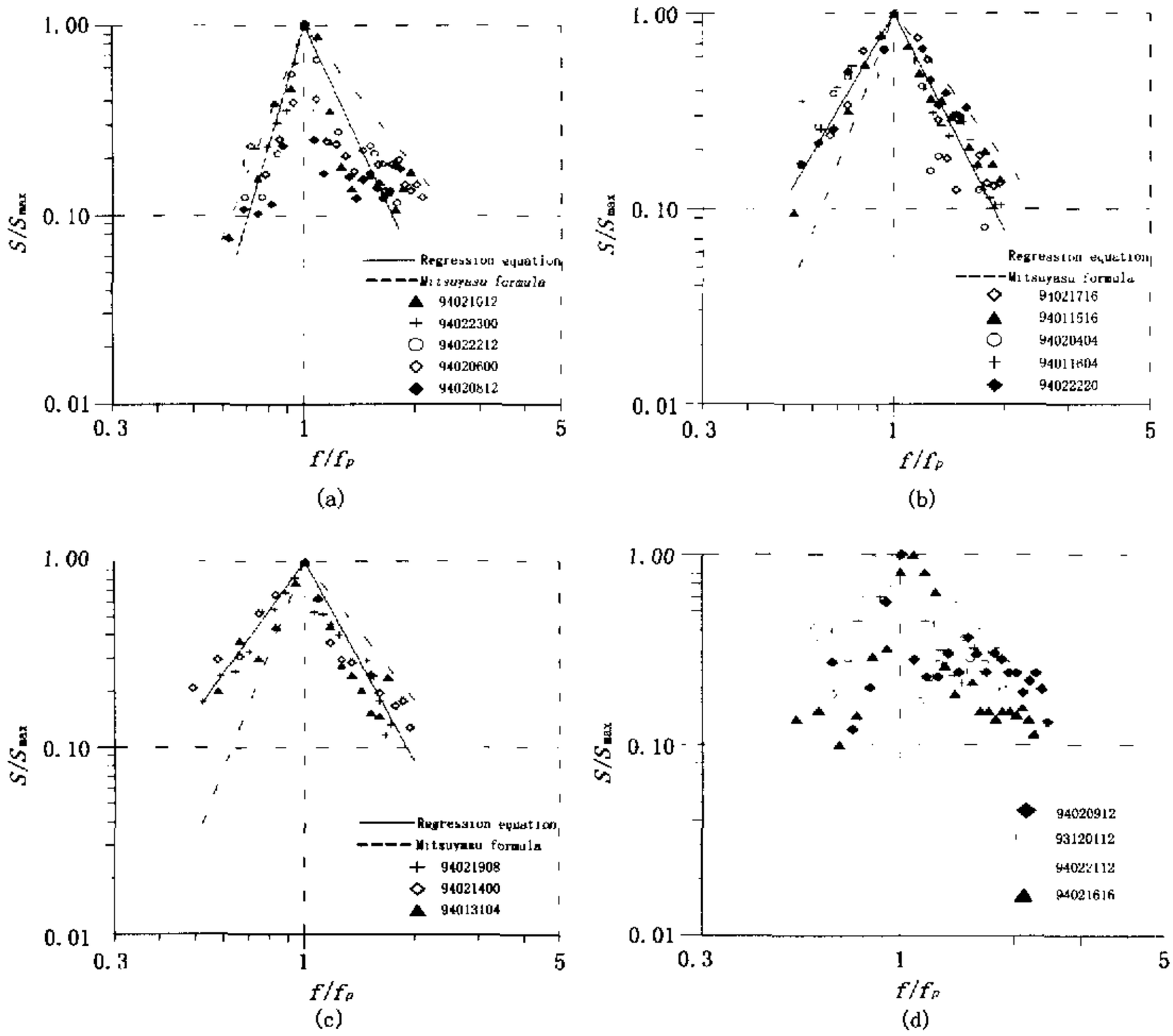

Fig. 9. Subgroups of distribution of normalized S on non-dimensional frequency.
(a) Data sets with wave age $3.0 < \zeta < 6.0$, (b) Data sets with wave age $1.5 < \zeta < 3.0$,
(c) Data sets with wave age $1.0 < \zeta < 1.5$, (d) Data sets with wave age $\zeta < 1.0$.

$$\frac{S}{S_{max}} = \begin{cases} (f/f_p)^a ; & f \leqslant f_p \\ (f/f_p)^b ; & f > f_p \end{cases}$$

$$\begin{cases} a = 0.91\zeta + 1.53 \\ b = -0.08\zeta + 3.51 \end{cases} ; \quad 1 < \zeta \leqslant 6 \tag{36}$$

in which ζ is the wave age.

To obtain the modified directional spreading model, the relationship between S_{max} and other sea state parameters art investigated. Mitsuyasu *et al*. showed that the parameter S_{max} could be a function of wave age, C_m/U. Based on the selected data sets, Fig. 12 shows that the relationship is scatter and the result is not so consistent with the empirical equation derived by Mitsuyasu *et al*. Therefore, the use of the wave age can not properly indicate the stage of monsoon-generated wave development in this area. Anoth-

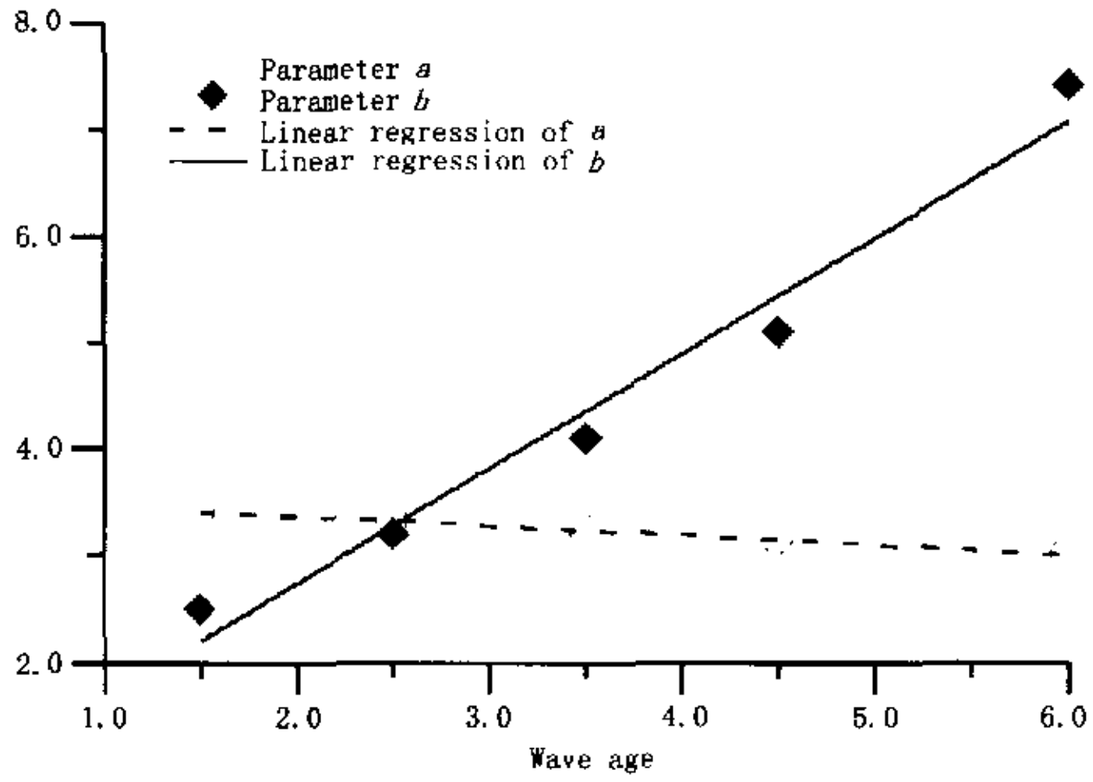

Fig. 10. Dependency of parameters a and b on wave age.

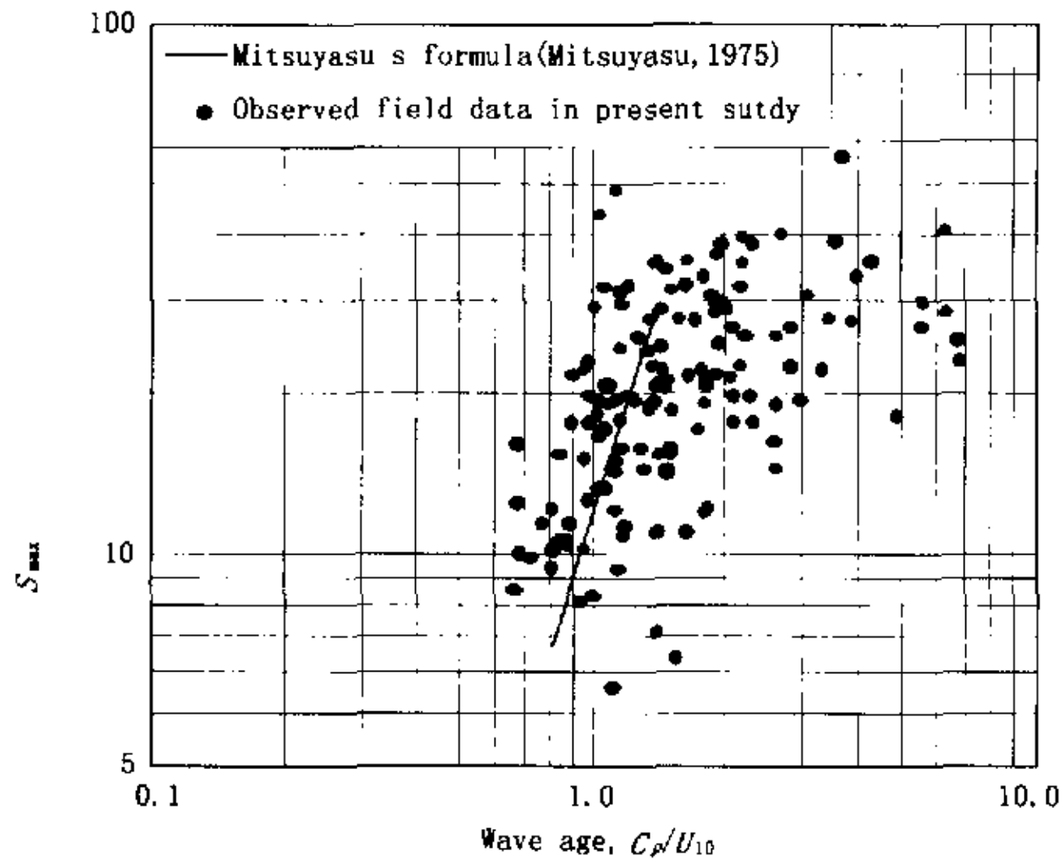

Fig. 11. Relationship between S_{max} and wave age.

er parameter for indicating the stage of wave development is wave steepness. Fig. 13 is the log-log plot of parameter S_{max} against wave steepness. It shows that the values of S_{max} decrease as the wave steepness increases. The relationship between S_{max} and wave steepness could then be approximately represented by an empirical equation

$$S_{max} = 0.26\left(\frac{H_s}{L_p}\right)^{-1.04}. \tag{37}$$

The correlation coefficient between Eq. (37) and the selected data is 0.78. The high correlation coefficient suggests that Eq. (37) and Eq. (36) may be a proper way to obtain the directional spectrum for engineering applications conveniently.

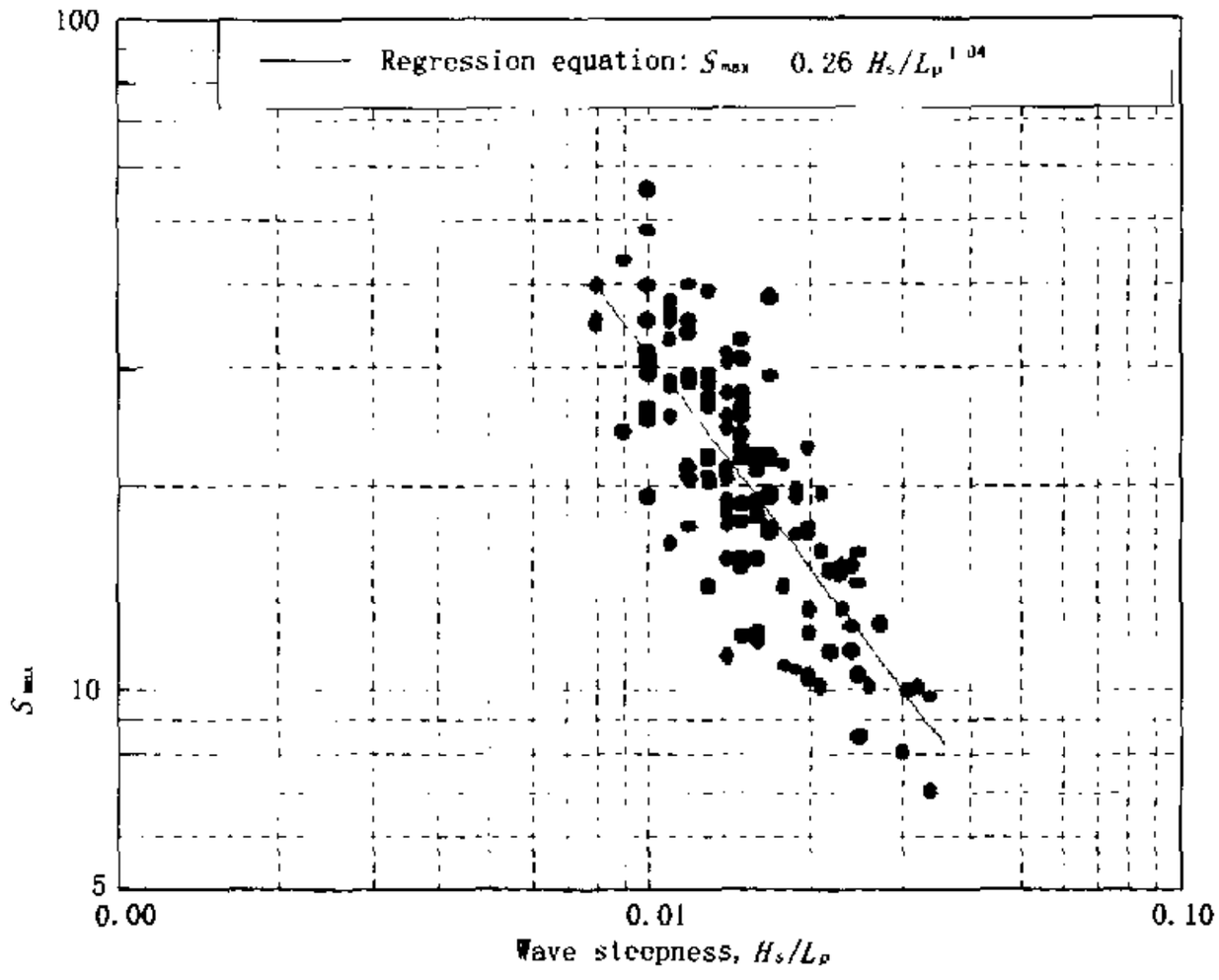

Fig. 12. Relationship between S_{max} and wave steepness.

4.3 Discussions

The directional spreading cosine power model, $\cos^{2S}$, originally proposed by Longuet-Higgins *et al*. (1963), is widely used due to its proven generality. The discussions of the characteristics of the model can be separated into two parts, i.e., the S_{max} and the behavior of S with respect to non-dimensional frequency.

S_{max}, which is the maximum spreading parameter of wave spectrum, is often used to represent the concentration of wave energy respect to a corresponding direction. It occurs at the peak frequency in most cases, however, analysis of field data collected during turning wind direction also demonstrates that S_{max} may also occur at the frequency at which the wave components are generated by the turning wind. S_{max} varies during wave evolution. Mitsuyasu *et al*. (1975) showed that S_{max} can be determined from the wave age, which is the ratio of wave phase speed to wind speed. This relationship of S_{max} and wave age and wave steepness is also checked and modified according to our data. S_{max} was recommended by Goda (1985) of a value of 10 for wind waves, 25 for swell with short decay, and 75 for swell with long decay distance. S_{max} is also related to the behavior of S_{ni} in finite depth.

On the other hand, the characteristics of directional spreading parameter S are not as clearly understood as those of S_{max}. In the present study, the characteristics of directional spreading parameter S with respect to non-dimensional frequency is estimated by BPEM, which simplifies the data fitting procedures and hence improves the validity. A modification of parameterization is proposed accordingly. The major difference between the present formulation and that by Mitsuyasu *et al*. (1975), Hasselmann *et al*. (1980), and Donelan(1985) lies in the dependency on the wave age. Based on their measuremens, the

wave age is not involved in Donelan's formula, while the Hasselmann's and Mitsuyasu's formulations are dependent on the wave age. The proposed formulation even exhibits more comprehensive relation to the wave age.

The wave age is an important parameter in describing the stage of wave growth. The dependency of directional spreading to the wave age under the stage of wave development has been discussed by Hasselmann *et al*. (1980) and Donelan *et al*. (1985). Young (1999) concluded that the answer is on whether the sea state is dominated by non-linear wave-wave interaction or atmospheric input process. At the stage of development of the wave the atmospheric input plays the major role, thus the directional spreading should be dependent on the wave age. If, however, the nonlinear wave-wave interaction, originally proposed by Hasselmann (1962), governs the situation, then the directional spreading should not be a function of wave age.

Young and Van Vledder (1993) and Banner and Young (1994) used numerical spectral model with full solution to the non-linear source term to investigate the nonlinear interaction of wind wave generation. They found that the atmospheric input plays a very minor part. And the nonlinear interaction controls the directional spreading. Therefore they suggested that the directional spreading should not be a function of wave age. Non- or weak wave age dependent formulations were recommended.

The conclusion of Young and Van Vledder (1993) and Banner and Young (1994) is based on the wave data with $C_p / U_{10} < 1$. It should be noted that the field data in the present study covers a wide range of wave age. Considering the steady monsoon wind state chosen for analysis, the waves neither oppose the wind direction nor overrun the wind. Certain part of the wave data, which has faster wave celerity than wind speed, could be regarded as swell. The present results demonstrate that the swell is influenced by the wind. The interaction between the waves and atmosphere may be an important factor concerning the wave spectral evolution. Since the detailed features of directional spectral development are not well modeled, further refinement of the description of spectral evolution is needed for better understanding of waves.

5. Summary and Conclusions

In the present paper, a new method, named the Bayesian Parameter Estimation Method(BPEM) is proposed. Instead of solving cross-spectral density matrix in conventional directional spectral analysis methods, the BPEM is to approach a chosen directional spreading function by fitting its parameters to a criterion derived from a Bayesian viewpoint. The BPEM could be considered as a regression analysis to find the maximum joint probability of parameters, which best approximates the observed data. By application of the transfer function to directional spectra the method can also be applied to directional wave analysis based on an arbitrary mixed instrument array measurement. In comparison, the BPEM is formulated *in the same manner* as *the Bayesian Approach Method*(BAM), *i.e.*, *considering errors in the cross-*spectra. However, instead of using complicated theoretical methodology and time-consuming iterative calculations in BAM, the simplicity and efficiency make the BPEM easy to apply for in-situ analysis. It also simplifies the sequences and lowers the possible accumulated errors induced by traditional procedures, in

which conventional directional spectrum analysis methods are performed and then the estimated directional spreading distributions are fitted to a chosen spreading model to have its corresponding parameters.

The local features of directional waves off Taishi coast in the winter monsoon season are investigated. Field data measured from a spatial array of wave gauges installed on an observation platform has been analyzed. The normalized directional spreading parameter S/S_{max} in the formula is derived as a function of f/f_p. The results show the same tendency as previous observations that directional concentration has the maximum value at the spectral peak and decreases at both sides of the spectral peak. However, it is found that the relationship between the normalized parameter S and the non-dimensional frequency of swell is influenced by wave age. Mitsuyasu's formula for directional spreading function is justified to be representative of wave field. The analysis of field data also shows that S_{max} can be expressed by an empirical formula, in which S_{max} is a function of wave steepness.

References

Bretthorst, G.L., 1988. Bayesian spectrum analysis and parameter estimation, *Maximum Entropy and Bayesian Methods in Science and Engineering*, **1**, 75 ~ 145.

Donelan, M.A., Hamilton, J. and Hui, W.H., 1985. Directional spectra of wind generated waves. *Phil. Trans. R. Soc.* London, A**315**, 509 ~ 562.

Goda, Y., 1985. *Random seas and design of marine structures*, University of Yokyo Press.

Hashimoto, N., Kobune, K. and Kameyama, Y., 1987. *Estimation of directional spectrum using the Bayesian approach and its application to field data analysis*, Rept. of the P.H.R.I., **26**(5).

Hashimoto, N. and Nagai, T., 1994. Extension of the maximum entropy principle method for directional wave spectrum estimation. *Proc. 25th Int. Conf. on Coastal Eng.* (ASCE), 232 ~ 246.

Hasselmann, E.E., Dunckel, M., and Ewing, J.A., 1980. Directional wave spectra observed during JONSWAP 1973, *J. Phys. Oceanogr.*, **10**, 1264 ~ 1280.

Hasselmann, K., 1962. On the non-linear energy transfer in a gravity -wave spectrum. Part 1. General Theory, *J. Fluid Mech.*, **12**, 481 ~ 500.

Isobe, M. and Horikawa, K., 1984. Extension of MLM for estimating directional wave spectrum, *Proc. Sympo. on Description and Modeling of Directional Seas*. Paper No. A-6

Jeffreys, H., 1961. *Theory of Probability*, Oxford University Press, London.

Kim, T., Lin, L.W. and Wang H., 1993. Comparisons of Directional Wave Analysis Methods, *Proc. of Second International Symposium of Ocean Wave Measurement and Analysis*, New Orleans, 554 ~ 568.

Longuet-Higgins, M.S., Cartwright, D.E. and Smith, N.D., 1963. Observations of the directional spectrum of sea wave using the motions of a floating buoy, *Proc. Conf. Ocean Wave Spectra*, Prentice -Hall Inc., 111 ~ 132.

Mitsuyasu, H., Tasai, F., Sunara, T., Mizuno, S., Onkusu, M., Honda, T. and Rukiiski, K., 1975. Observations of the directional spectrum of ocean waves using a cloverleaf buoy, *J. Phys. Oceanogr.*, **5**, 751 ~ 761.

Young, I.R. and Van Vledder, G.Ph., 1993. The central role of nonlinear interactions in wind-wave evolution, *Philos. Trans. R. Soc. Lond.*, A**342**, 505 ~ 524.

Young, I.R., 1999. *Wind gererated ocean waves*, Elsevier press.